Empirical bond polarizability model for fullerenes

S. Guha, J. Menéndez, J. B. Page, and G. B. Adams
Department of Physics and Astronomy, Arizona State University, Tempe, Arizona 85287-1504
(Received 8 December 1995)

The static polarizability properties and the Raman-scattering intensities in molecular C_{60} and C_{70} are found to be well reproduced by a bond polarizability model with parameters similar to those obtained from studies of hydrocarbons. For the Raman spectrum of C_{60} with off-resonance infrared laser excitation, a fit using first-principles vibrational eigenvectors yields $\alpha_\parallel'-\alpha_\perp'=2.30$ Å^2, $2\alpha_\perp'+\alpha_\parallel'=2.30$ Å^2, $\alpha_\parallel-\alpha_\perp=1.28$ Å^3 for single bonds and $\alpha_\parallel'-\alpha_\perp'=2.60$ Å^2, $2\alpha_\perp'+\alpha_\parallel'=7.55$ Å^2, $\alpha_\parallel-\alpha_\perp=0.32$ Å^3 for double bonds, with $(\alpha_\parallel-\alpha_\perp)$ for the single bond arbitrarily set equal to its value in ethane, namely, 1.28 Å^3. The transferability of these parameters to C_{70} is discussed in detail. [S0163-1829(96)07119-4]

I. INTRODUCTION

The discovery of a method for the production of large quantities of fullerenes[1] allowed the study of these materials using standard characterization techniques. In particular, Raman spectroscopy has provided a wealth of information on symmetry,[2,3] disorder,[4–6] structural transitions,[7] electronic structure,[8–10] and the effects of irradiation[11] and doping.[12,13] Most of these studies have concentrated on the well-known Buckminsterfullerene C_{60}, but Raman scattering is also a powerful technique for the study of other fullerene-based materials (such as polymerized fullerenes or fullerene fibers), the detailed structures of which remain unknown.[14] Proposed structures for these materials can be verified spectroscopically to a great extent, if their Raman spectra can be predicted. This involves not only the accurate calculation of vibrational frequencies, but also the prediction of the corresponding Raman intensities. Recent advances in *ab initio* techniques make it possible to obtain very accurate vibrational frequencies and mode displacement patterns for covalent systems.[15–18] Moreover, some of the first-principles methods can be extended to predict off-resonance Raman intensities.[15] However, such calculations can be computationally very intensive and less accurate than the purely vibrational applications, and it is therefore desirable to develop an empirical method for the calculation of Raman intensities in fullerenes. Recently, Snoke and Cardona[19] have shown that satisfactory agreement with the experimental Raman spectrum of C_{60} can be obtained within a simple bond polarizability model. This result is significant, because previous studies suggest that the bond polarizabilities for carbon-carbon bonds are transferable,[20] so that polarizability parameters obtained for C_{60} might be useful for the prediction of Raman spectra of other fullerenes. It was noted by Snoke and Cardona,[19] however, that their polarizability parameters fit to C_{60} are very different from the values obtained for carbon-carbon bonds in hydrocarbons,[21–23] raising doubts as to the transferability of carbon-barcon bond polarizability parameters to fullerenes.

In this paper, we show that the static polarizability properties of fullerenes can be understood in terms of hydrocarbon bond polarizabilities within the framework of a bond polarizability model. In addition, using mode eigenvectors obtained from first-principles calculations, together with hydrocarbon polarizability parameters, we calculate the Raman spectrum of C_{60} and C_{70} and find qualitative agreement with measured spectra obtained using off-resonance infrared excitation.[24] A marked improvement for C_{60} is then obtained for a bond polarizability fit to the experimental Raman intensities. The resulting fit parameters are closer to the hydrocarbon values than those obtained from earlier fits to Raman spectra obtained with visible excitation.[19] We analyze in detail the difference between the hydrocarbon parameters and our fit parameters and discuss their transferability to C_{70}.

II. BOND POLARIZABILITY MODEL FOR THE STATIC POLARIZABILITY OF FULLERENES

A simple model for the static electronic polarizability of a molecule[25] postulates that this quantity can be expressed as a sum of individual bond polarizabilities, which are assumed to be roughly independent of the chemical environment, i.e., transferable between different compounds. The bond polarizability for a given pair of atoms can be written as the sum of an isotropic and an anisotropic tensor:

$$\Pi_{\alpha\beta}=\tfrac{1}{3}(\alpha_\parallel+2\alpha_\perp)\delta_{\alpha\beta}+(\alpha_\parallel-\alpha_\perp)\left(\frac{R_\alpha R_\beta}{R^2}-\tfrac{1}{3}\delta_{\alpha\beta}\right), \qquad (1)$$

where α and β are Cartesian coordinates and $\mathbf{R}$ is the vector connecting the two atoms linked by the bond. The assumption here of cylindrical symmetry around the principal axis of the bond is consistent with the transferability hypothesis, since any deviation from cylindrical symmetry would be due to the effect of the chemical environment on an individual bond.

The mean static molecular polarizability $\overline{\alpha}$, defined as $\overline{\alpha}=\frac{1}{3}(\alpha_{xx}+\alpha_{yy}+\alpha_{zz})$, is given by the sum of the mean polarizabilities $\overline{\Pi}=\frac{1}{3}(\Pi_{xx}+\Pi_{yy}+\Pi_{zz})\equiv\frac{1}{3}(\alpha_\parallel+2\alpha_\perp)$ for all bonds in the molecule. Experimentally, there is considerable evidence for the transferability of these mean bond polarizabilities.[26] Other parameters, such as the bond anisotropies $\alpha_\parallel-\alpha_\perp$ or the derivatives of the bond polarizabilities with respect to the bond lengths, have not been found to be equally transferable, particularly for C—H bonds.[23,26] On the other hand, an attempt by Bermejo and

co-workers[20] to transfer polarizability parameters from the C—C single bond in ethane to diamond was quite successful, suggesting that it might be possible to describe carbon-carbon bonds in terms of transferable polarizabilities. The recent availability of fullerenes provides an ideal system to test this hypothesis.

The experimental mean polarizability of C_{60} is $\overline{\alpha}=83$–85 Å^3 (Refs. 27 and 28). We will now show that this value is consistent with the transferability hypothesis if we associate the ''single bonds'' in C_{60} with the C—C single bond in ethane (C_2H_6) and the ''double bonds'' in C_{60} with the C═C double bond in ethylene (C_2H_4), as proposed by Snoke and Cardona.[19] We can obtain the mean polarizability Π of the carbon-carbon bonds in these hydrocarbons, if we assume that the mean polarizabilities of their C-H bonds are also transferable. For these we will use methane (CH_4). From the experimental value for the mean polarizability of methane, $\overline{\alpha}_{CH_4}=2.59$ Å^3 (Ref. 29), we obtain $\frac{1}{3}(\alpha_\parallel+2\alpha_\perp)^{C-H}=\frac{1}{4}\times(2.59)=0.648$ Å^3. Assuming this same value for the mean polarizability of the C—H bond in ethane, and using the experimental mean molecular polarizability $\overline{\alpha}_{C_2H_6}=4.56$ Å^3 (Ref. 30), we obtain for the C—C single bond in this molecule $\frac{1}{3}(\alpha_\parallel+2\alpha_\perp)^{C-C}=4.56$ Å$^3-6\times0.648$ Å$^3=0.672$ Å^3. Next, we extract the mean polarizability of the C═C double bond from the measured polarizability of ethylene, using the same procedure. From the experimental mean molecular polarizability $\overline{\alpha}_{C_2H_4}=4.22$ Å^3 (Ref. 31), we obtain $\frac{1}{3}(\alpha_\parallel+2\alpha_\perp)^{C=C}=4.22$ Å$^3-(4\times0.648$ Å$^3)=1.63$ Å^3. In C_{60}, there are 60 single bonds and 30 double bonds, so that the bond polarizability model predicts $\overline{\alpha}=(60\times0.672$ Å$^3)+(30\times1.63$ Å$^3)=89.2$ Å^3, in excellent agreement with the experimental value and with the value predicted by local-density approximation calculations.[32,15]

We next turn to C_{70}, for which the experimental mean polarizability is $\overline{\alpha}=94$ Å^3 (Refs. 33 and 34). There are eight distinct bonds in this molecule. However, since the individual bond polarizability parameters are not available for each of these, we make the simplifying assumption that the C_{70} bonds can be partitioned into a ''single-bond'' group and a ''double-bond'' group, and use the C_{60} polarizability parameters to compute $\overline{\alpha}$. The best agreement with the experimental mean molecular polarizability is found when the cutoff bond length between the two groups is taken as 1.425 Å^3, midway between the single and double-bond lengths in C_{60}. This yields a calculated mean molecular polarizability $\alpha=109.2$ Å^3. The 1.425-Å^3 cutoff assigns single-bond character to all pentagon bonds, as in C_{60}, and to the longest hexagon bond, which is also the longest bond in C_{70}. We will show below that this choice also leads to the best agreement between the predicted and experimental Raman spectrum.

Calculations by Wang, Bertsch, and Tománek[35] suggest that the polarizability of C_{60} is strongly dependent on ''screening'' effects. On the other hand, the results of Bermejo *et al.*[20] indicate that local-field corrections are essential if one transfers the ethane C—C polarizability to the C—C bonds in diamond. For C_{60}, the good agreement we find without these corrections indicates that they may not be important. It should be noted, however, that the C—C single bond lengths in ethane and C_{60} differ by 6%. Hence these bonds are not identical, and it is possible that by transferring the ethane C—C polarizability to C_{60}, we have included screening in some effective manner. We will return to this topic when discussing the Raman polarizability parameters.

III. BOND POLARIZABILITY MODEL FOR THE RAMAN SPECTRA OF FULLERENES

A. Transferability of Raman polarizability parameters from hydrocarbons to C_{60} and C_{70}

The bond polarizability model can be extended to the calculation of Raman-scattering intensities.[36] The intensity of first-order off-resonance Stokes Raman scattering for a harmonic system can be written as

$$I_{\eta'\eta}(\omega)=C\omega_L\omega_S^3\sum_{f=1}^{3N}\frac{\langle n(\omega_f)\rangle+1}{\omega_f}\left|\sum_{\alpha\beta}\eta'_\alpha\eta_\beta P_{\alpha\beta,f}\right|^2\times\delta(\omega-\omega_f). \tag{2}$$

Here, C is a frequency-independent constant; ω_L and ω_S are the incident and scattered light frequencies, respectively; $\omega\equiv\omega_L-\omega_S$ is the Raman shift; η and η' are unit vectors along the incident and scattered polarization directions, respectively; $\langle n(\omega_f)\rangle\equiv[\exp(\beta\hbar\omega_f)-1]^{-1}$ is the thermal average occupation number of mode f at temperature $T=(k_B\beta)^{-1}$; and the quantity $P_{\alpha\beta,f}$ is the derivative of the electronic polarizability tensor with respect to the normal coordinate for mode f. Hence the calculation of the Raman spectrum requires mode frequencies, mode eigenvectors, and polarizability derivatives. In terms of the mode eigenvectors, $P_{\alpha\beta,f}$ is given by

$$P_{\alpha\beta,f}=\sum_{l\gamma}\left[\frac{\partial P_{\alpha\beta}}{\partial u_\gamma(l)}\right]_0\chi_\gamma(l|f), \tag{3}$$

where $\{[\partial P_{\alpha\beta}/\partial u_\gamma(l)]_0\}$ are the electronic polarizability derivatives with respect to the real-space atomic displacements $\{u_\gamma(l)\}$, evaluated at the system's equilibrium configuration. Here, $l=1,N$ labels the atomic sites and $\gamma=1,3$ labels Cartesian components. The mode eigenvectors $\boldsymbol{\chi}(f)$ are obtained from the $3N\times3N$ matrix eigenvalue problem $(\boldsymbol{\Phi}-\omega_f^2\mathbf{M})\boldsymbol{\chi}(f)=0$, subject to the orthonormality condition $\Sigma_{l\alpha}\chi_\alpha(l|f)\chi_\alpha(l|f')m_l=\delta_{ff'}$, where m_l is the mass of atom l and the sum is over all sites and directions. The force-constant matrix is $\boldsymbol{\Phi}$, and the elements of the mass matrix $\mathbf{M}$ are $M_{\alpha\beta}(l,l')=m_l\delta_{ll'}\delta_{\alpha\beta}$.

In order to evaluate the derivatives in Eq. (3), it is customary to adopt the bond polarizability model of Eq. (1) and make the additional assumption, known as the ''zero-order approximation,'' [37] that the bond polarizability parameters are functions of the bond lengths R only, i.e., $\alpha_\parallel\equiv\alpha_\parallel(R)$ and $\alpha_\perp\equiv\alpha_\perp(R)$. This approximation neglects the dependence of a bond's polarizability on the motion of atoms not connected to that bond. The equilibrium-configuration derivatives of the polarizability with respect to the atomic displacements $\{u_\gamma(l)\}$ are then easily linked to derivatives with respect to the γ components of the three-dimensional bond vectors $\{\mathbf{R}(l,B)\}$ from atom l to neighboring atoms B. Giving atom l a displacement $\mathbf{u}(l)$ and keeping all other atoms fixed at their equilibrium positions, we have $\mathbf{R}(l,B)=\mathbf{R}_0(l,B)-\mathbf{u}(l)$,

where $\mathbf{R}_0(l,B)$ is the equilibrium bond vector from atom l to atom B. It is then straightforward to obtain $P_{\alpha\beta,f}$ as a sum of three contributions:

$$P_{\alpha\beta,f} = -\sum_l \sum_B \left[\left(\frac{\alpha'_\parallel(B) + 2\alpha'_\perp(B)}{3} \right) \mathbf{R}_0(l,B) \cdot \boldsymbol{\chi}(l|f) \delta_{\alpha\beta} + [\alpha'_\parallel(B) - \alpha'_\perp(B)][\hat{R}_{0\alpha}(l,B)\hat{R}_{0\beta}(l,B) - \tfrac{1}{3}\delta_{\alpha\beta}]\mathbf{R}_0(l,B) \cdot \boldsymbol{\chi}(l|f) + \left(\frac{\alpha_\parallel(B) - \alpha_\perp(B)}{R_0(l,B)} \right) \times \{\hat{R}_{0\alpha}(l,B)\hat{\chi}_\beta(l|f) - \hat{R}_{0\beta}(l,B)\hat{\chi}_\alpha(l|f) - 2\hat{R}_{0\alpha}(l,B)\hat{R}_{0\beta}(l,B)[\mathbf{R}_0(l,B) \cdot \boldsymbol{\chi}(l|f)]\} \right], \quad (4)$$

Here, the primes denote radial derivatives, the carets denote unit vectors, and the sum over B extends over the bonds connected to site l. The first term in Eq. (4) represents the change in the isotropic part of the polarizability induced by bond stretching, and the second term represents the corresponding change in the anisotropic part of the polarizability. The third term in Eq. (4) corresponds to the change in the anisotropic part of the polarizability induced by bond rotations. In C_{60}, the two A_g modes contribute to the first term, and the eight H_g modes contribute to the other two. Since bond stretching is associated with larger restoring forces, we expect the high-energy H_g modes to contribute preferentially to the second term in Eq. (4), whereas the low-energy H_g modes should make a larger contribution to the third term.

For C_{60}, the sum over bonds in Eq. (4) includes two types of bonds, single and double, so there are six independent parameters that determine the Raman intensities. For C_{70}, which has eight distinct bonds, there are 24 such parameters. In view of the success of the transferability scheme for the prediction of the static polarizability of molecular C_{60} and C_{70}, we now investigate the transferability of hydrocarbon parameters for the description of their Raman spectra. In analogy with the static polarizability calculations, we use for the single bonds in C_{60} the Raman polarizability parameters for the C—C single bond in ethane,[22] and for the double bond in C_{60}, we use the Raman polarizability parameters for the double bond in ethylene.[23] Since the ethylene molecule is planar, the anisotropy $\alpha_\parallel - \alpha_\perp$ of its C═C double-bond polarizability lacks cylindrical symmetry. Accordingly, following Snoke and Cardona, we use the average of the polarizability anisotropies for the two inequivalent directions perpendicular to the principal axis of the ethylene molecule, as determined by Orduna *et al.*[23] The hydrocarbon Raman polarizability parameters that we have used are listed in the last column of Table I. For C_{70}, there is no hydrocarbon analog for each of the eight distinct bonds, as pointed out in Sec. II. An interpolation between ethane and ethylene parameters as a function of the C_{70} bond lengths might be attempted, but the resulting differences between some of the parameters would be of the order of the expected ''first-order'' terms,[22] or comparable with the deviations from cylindrical symmetry observed for hydrocarbons.[23] Hence, the physical validity of any improvement in the predicted spectra might be questionable. We thus adopt the same procedure used to compute the static polarizability of C_{70}: we partition the C_{70} bonds into two groups, and assign hydrocarbon single-bond Raman polarizability parameters to the group with longer bonds and hydrocarbon double-bond Raman polarizability parameters to the group with shorter bonds. The cutoff between the two groups is chosen so that we obtain the best possible agreement with the experimental Raman spectrum. It is important to point out that our study is limited to a comparison of *ratios* of predicted and experimental intensities, since no absolute Raman intensity measurements for fullerenes are available in the literature. Therefore, we can only study the transferability of *ratios* of bond polarizability parameters.

TABLE I. Raman polarizability parameters for C_{60}. As discussed in the text, the static polarizability anisotropy $\alpha_\parallel - \alpha_\perp$ for the single bond was arbitrarily set equal to 1.28 Å^3, which is its value in ethane. The first column lists the polarizability parameters, which we obtain from fits to the experimental off-resonance Raman spectrum of Chase, Herron, and Holler (Ref. 24). The second column gives the polarizability parameters of C_{60} from Ref. 19, and the last column lists the experimental polarizability parameters in hydrocarbons for the C—C single bond in ethane (Ref. 22) and the C═C double bond in ethylene (Ref. 23).

	Fit values	Snoke and Cardona[a]	Hydrocarbons
Single bonds			
$(\alpha'_\parallel - \alpha'_\perp)$	(2.30±0.30) Å^2	(1.35±0.20) Å^2	2.31 Å^2 [b]
$(2\alpha'_\perp + \alpha'_\parallel)$	(2.30±0.01) Å^2	(1.28±0.30) Å^2	3.13 Å^2 [b]
$(\alpha_\parallel - \alpha_\perp)$[c]	(1.28) Å^3 [c]	(1.28±0.20) Å^3	1.28 Å^3 [b]
Double bonds			
$(\alpha'_\parallel - \alpha'_\perp)$	(2.60±0.36) Å^2	(4.50±0.50) Å^2	2.60 Å^2 [d]
$(2\alpha'_\perp + \alpha'_\parallel)$	(7.55±0.40) Å^2	(5.40±0.70) Å^2	6.50 Å^2 [d]
$(\alpha_\parallel - \alpha_\perp)$	(0.32±0.09) Å^3	(0.00±0.20) Å^3	1.65 Å^3 [d]

[a]From Ref. 19.
[b]From Ref. 22.
[c]Set equal to the C—C single-bond value for ethane, as discussed in the text.
[d]From Ref. 23.

In addition to the polarizability parameters, the calculation of Raman intensities from Eq. (4) requires mode eigenvectors. In the case of tetrahedral semiconductors, the lattice dynamics of which have been exhaustively studied, mode eigenvectors predicted from empirical models are in poor agreement with inelastic-neutron-scattering experiments, even for models which are very successful in reproducing the mode *frequencies*. On the other hand, *ab initio* calculations are in good agreement with experimental measurements of both frequencies and eigenvectors.[38] In the case of C_{60}, we have found that *ab initio* calculations by Giannozzi and Baroni[15] and Adams *et al.*[16] yield virtually identical eigenvectors, even though their predicted frequencies differ by as much as 7%. We use these eigenvectors in Eq. (4). For C_{70}, we use first-principles vibrational eigenvectors from Adams, Page, and Sankey.[39]

Calculated Raman intensities for C_{60} and C_{70} using Eq. (4), first-principles eigenvectors, and the polarizability parameters given in the third column in Table I, are compared with experimental data in Figs. 1 and 2, respectively. The bond polarizability model is expected to break down when resonance effects become important, i.e., for excitation ener-

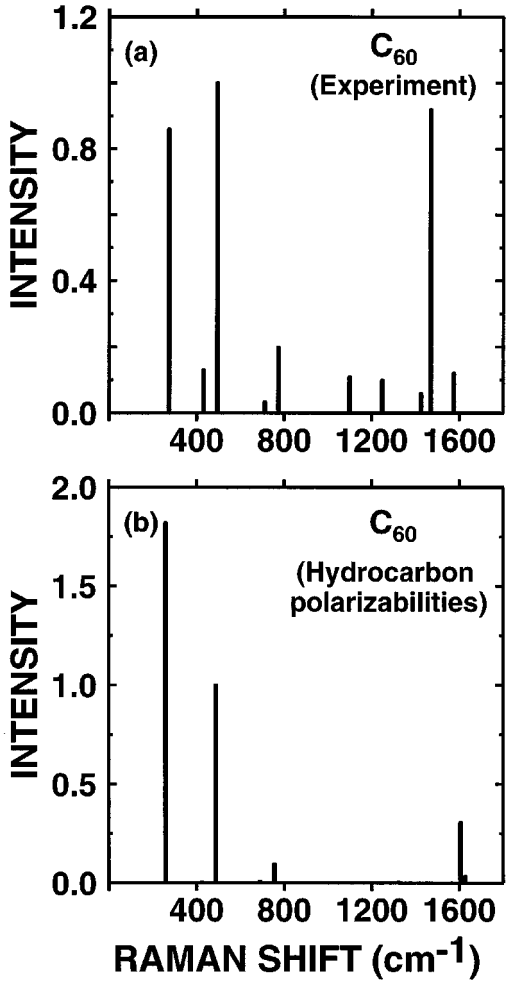

FIG. 1. (a) Experimental Raman intensities of C_{60} obtained by Chase, Herron, and Holler in Ref. 24. (b) Calculated intensities of the Raman-active modes in C_{60}, using the bond polarizability model. We have used the polarizability parameters of hydrocarbons (Refs. 22 and 23), together with first-principles eigenvectors and eigenfrequencies of Adams *et al.* (Ref. 16). In both (a) and (b), the Raman intensities have been normalized to the experimental $A_g(1)$ mode at 493 cm^{-1}.

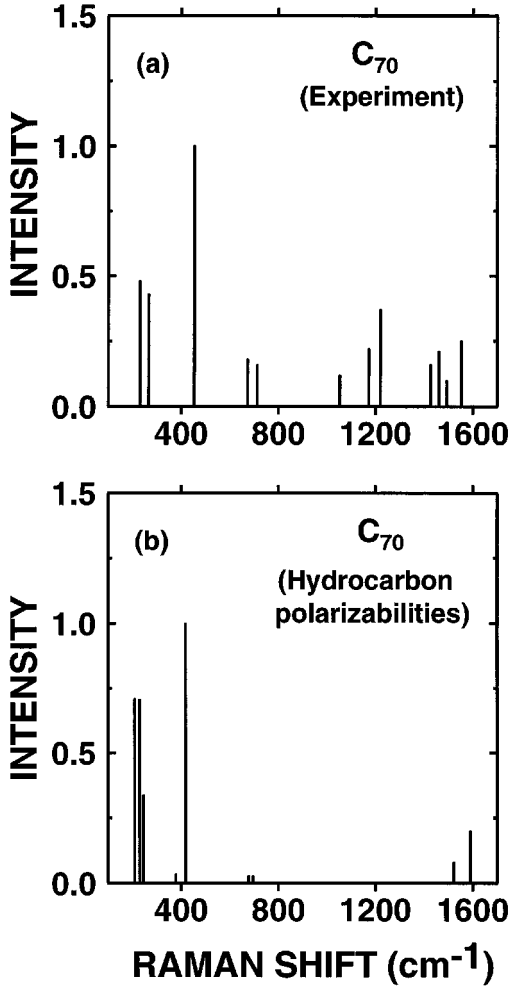

FIG. 2. (a) Experimental Raman intensities for C_{70}, obtained by Chase, Herron, and Holler in Ref. 24. (b) Calculated intensities of the Raman-active modes in C_{70}, using the bond polarizability model with the polarizability parameters of hydrocarbons (Refs. 22 and 23) and first-principles eigenvectors and eigenfrequencies of Adams, Page, and Sankey (Ref. 39). The symmetry is D_{5h} and the irreducible representations labeling the peaks follow the notation of Ref. 40. In both (a) and (b), the intensities have been normalized to the A_1' mode at 400 cm^{-1}.

gies near or above the band gap,[10] which for C_{60} and C_{70} lie in the range of visible excitation. Accordingly our comparison with experiments are based on Raman spectra obtained by Chase, Herron, and Holler,[24] using an incident wavelength of 1064 nm. We expect these spectra to be less affected by resonance effects than the original Raman data from Bethune *et al.*,[2] which were obtained using the 514-nm line of an Ar^+ laser.

The predicted and experimental Raman spectra in Figs. 1 and 2 show both significant agreements and discrepancies. For the case of C_{70}, it is interesting that we find the best agreement between the predictions and experiment for a cutoff length of 1.425 Å between ''single'' and ''double'' bonds. This is exactly the same as that found to give the best agreement for the static polarizability of the molecule. As noted earlier, this cutoff is midway between the single- and double-bond lengths in C_{60}.

The strongest peaks in the predicted spectra of Figs. 1 and 2 are seen to be strong in the experimental Raman spectra. It should also be noted that the three low-energy peaks predicted by our calculation for C_{70} are indeed observed in higher-resolution experiments.[24] The relative intensity between the C_{60} ''squashing'' mode $H_g(1)$ at 270 cm^{-1} and the C_{60} ''breathing'' mode $A_g(1)$ at 493 cm^{-1}, and the relative intensity between their C_{70} counterparts, agree with experiment to within a factor of 2 or better. As will be shown below, these modes depend on different polarizability parameters, so that this good agreement with experiment indicates a partial success of the transferability scheme. On the other hand, the predicted intensities of the high-energy peaks relative to the low-energy peaks is not correct. For example, the ''pentagonal pinch'' $A_g(2)$ mode in C_{60} is predicted to be six times weaker than $H_g(1)$, whereas the corresponding experimental ratio is of order unity. Also, the weaker H_g peaks in C_{60}, as well as most of the medium-intensity peaks in C_{70}, are predicted to be much weaker than they appear in experiments.

The discrepancies between experiment and the bond polarizability model predictions using hydrocarbon parameters are not entirely surprising. The ''zero-order'' and cylindrical symmetry approximations that we have used fail to give perfect agreement with the Raman spectra of hydrocarbons, even when the polarizability parameters are simply fit to experimental data.[22] Furthermore, the transferability of the Raman polarizability parameters, particularly the anisotropy components in the third term of Eq. (4), is much more controversial than the transferability of the mean bond polarizabilities used to compute the mean static molecular polarizability.[21,26] Also, our calculated spectra correspond to isolated icosahedral molecules, which are isotopically pure, whereas the experimental data have been obtained from polycrystalline films. Thus, the experimental Raman intensities could be affected by intermolecular interactions in the solid phase and by the natural distribution of isotopes. In fact, the measured depolarization ratios for most of the H_g Raman peaks in C_{60} disagree with the value of 0.75 expected from icosahedral symmetry,[2] and none of the observed high-energy Raman peaks in C_{70} which have been tentatively assigned to the totally symmetric representation have a depolarization ratio close to zero.[24,41] The effect of isotopes can be estimated by recalculating the mode eigenvectors and eigenfrequencies for molecules with ^{13}C isotopes,[42] and we find this effect to be negligible.[43] On the other hand, solid-state effects are difficult to quantify and must be kept in mind as possible sources of the deviations between the calculated and observed spectra. In this regard, however, a microscopic calculation of bond polarizability parameters for molecular C_{60} by Sanguinetti and co-workers,[44] as well as a first-principles calculation of Raman intensities in molecular C_{60} by Giannozzi and Baroni,[15] are found to be in much better agreement with experiment than the results in Fig. 1, suggesting that the discrepancies in Figs. 1 and 2 are mostly due to the inadequacy of the bond polarizability model with hydrocarbon parameters and are not due to solid-state effects.

B. Bond polarizability model fit to the Raman spectrum of C_{60}

In order to ascertain the limits of the bond polarizability model, we have performed a fit of the Raman polarizability parameters to the Raman spectrum of C_{60}. A similar fit to C_{70} cannot be performed at this time, because its 53 possible Raman peaks have not been identified unambiguously. However, it is interesting to investigate the extent to which the use of Raman polarizability parameters obtained by simply fitting the C_{60} spectrum affect the agreement between predicted and experimental C_{70} Raman spectrum.

Snoke and Cardona[19] have previously fit a bond polarizability model to the C_{60} Raman spectrum obtained under near-resonance visible laser excitation.[2] For the vibrational mode eigenvectors and eigenfrequencies, they used a force-constant model which includes interactions up to second neighbors. Our fit differs from that of Ref. 19 in that we use first-principles eigenvectors and fit to experimental Raman data obtained with off-resonance near-infrared excitation. Experimental determinations of the absolute Raman intensities are rare and are not available for C_{60}, so that one of the six fitting parameters is absorbed into an undetermined overall scaling factor. The remaining five fitting parameters are

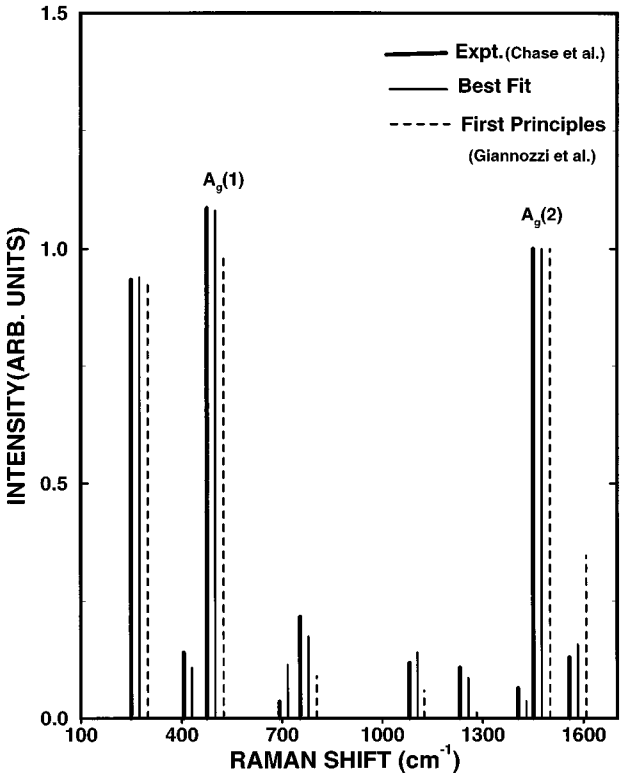

FIG. 3. Experimental and predicted normalized Raman spectra of C_{60}. The intensity of the $A_g(2)$ line at 1470 cm^{-1} has been set equal to unity, and the calculated lines have been shifted from the experimental frequencies by a small amount, for clarity. The thick solid lines represent the experimental data of Chase, Herron, and Holler (Ref. 24), and the thin solid lines show the fit obtained from the polarizability parameters in Table I. The dashed lines give the intensities predicted by *ab initio* calculations (Ref. 15). The *ab initio* predicted intensities of $H_g(2)$, $H_g(3)$, and $H_g(7)$ are vanishingly small.

thus ratios, and for convenience, we will express them in units of the measured static polarizability anisotropy $\alpha_{\|}-\alpha_{\perp}=1.28$ Å^3 for C—C single bonds in ethane. We find that this parameter gives the dominant contribution to the intensity of the $H_g(1)$ peak, so that its value in C_{60} could be determined directly by measuring this mode's absolute intensity, provided the constant C in Eq. (4) were known. In this paper, however, we compute only relative intensities.

We thus have a five-parameter model to fit the observed intensities for the ten first-order Raman active modes of C_{60}. Figure 3 shows the results of our best fit to the experimental Raman intensities in C_{60}. For comparison, the figure also includes the *ab initio* Raman intensities computed by Giannozzi and Baroni.[15] The polarizability parameters for our best fit are given in Table I. The largest source of error is the variation in the set of measured relative Raman intensities between experimental runs. We have estimated this error by performing a fit to a second Raman spectrum for near-infrared incident light, kindly provided by Dr. B. Chase. The differences between the polarizability parameters from these two fits result in the error estimates listed in Table I. Our fit parameters are seen to be quite close to the values determined for C—C and C═C bonds in hydrocarbons,[21–23] as listed in Table I. The key changes for the substantial im-

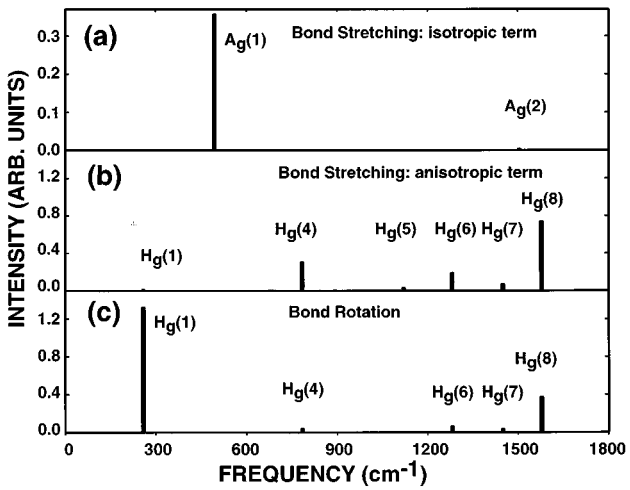

FIG. 4. Raman peak intensities in C_{60}, as computed from the three individual terms in Eq. (4). In each case, the nonzero polarizability parameters for the single and double bonds were set equal to unity. Panel (a) gives the contribution from the first term in Eq. (4). Panel (b) gives the intensities due to the second term in Eq. (4), and panel (c) shows the contribution from the last term. Notice that the total intensity is *not* the sum of those in the three panels, due to interference effects, as discussed in the text.

provement of Fig. 3 relative to Fig. 1 occur for the anisotropy ratio $[\alpha_{\parallel}(s)-\alpha_{\perp}(s)]/[\alpha_{\parallel}(d)-\alpha_{\perp}(d)]$ and the trace derivative ratio $[2\alpha'_{\perp}(s)+\alpha'_{\parallel}(s)]/[2\alpha'_{\perp}(d)+\alpha'_{\parallel}(d)]$. Compared to the values of these ratios in hydrocarbons, the former is smaller in C_{60}, and the latter is four times larger. We also note from Table I that while the ratio of the trace derivatives has changed, the weighted average of these derivatives (taking into account the fact that there are 60 single bonds and 30 double bonds) remains roughly constant, whereas the average value of the bond anisotropy becomes obviously smaller. The fit values obtained by Snoke and Cardona show the same trends, although the disagreements with hydrocarbon values are larger.

To gain a deeper insight into the significance of the differences between the hydrocarbon parameters and the fit parameters, we next look at the separate contributions to the Raman intensities from the three different terms in Eq. (4). The results are shown in Fig. 4. For each panel, the nonzero single- and double-bond parameters have been set equal to 1. It is important to keep in mind that the total Raman intensity is not the sum of the panels in Fig. 4, since the three terms in Eq. (4) must be added before squaring in Eq. (2) to compute the scattered intensity.

Figure 4(a) shows the contribution from the isotropic part of the polarizability, to which only the two totally symmetric A_g modes contribute. It is apparent that the relative intensity between the two A_g peaks is very different from the experimental value. The $A_g(1)$ peak is almost 100 times stronger than the $A_g(2)$ peak, whereas the experimental ratio is of order unity. This can be readily understood by inspection of the mode eigenvectors. For the $A_g(1)$ mode, the atomic displacements are essentially purely radial. Hence, the products $\mathbf{R}_0(lB)\cdot\boldsymbol{\chi}(l)$ in Eq. (4) have the same sign for all three bonds connected to any given atom. On the other hand, the atomic displacements for the ''pentagonal pinch'' $A_g(2)$ mode are essentially purely tangential. Hence, $\mathbf{R}_0(lB)\cdot\boldsymbol{\chi}(l)$ has opposite signs for single and double bonds. When the contributions from the three neighbors are added, a near cancellation occurs that accounts for the results shown in Fig. 4. This near cancellation is lifted if the polarizability parameter $[2\alpha'_{\perp}(B)+\alpha'_{\parallel}(B)]$ is different for single and double bonds. Hence, the relative intensities of $A_g(1)$ and $A_g(2)$ depend critically on the ratio $[2\alpha'_{\perp}(s)+\alpha'_{\parallel}(s)]/[2\alpha'_{\perp}(d)+\alpha'_{\parallel}(d)]$. To fit the experimental intensity ratio, we need $[2\alpha'_{\perp}(s)+\alpha'_{\parallel}(s)]/[2\alpha'_{\perp}(d)+\alpha'_{\parallel}(d)]=0.3$, which is smaller than the value $[2\alpha'_{\perp}(s)+\alpha'_{\parallel}(s)]/[2\alpha'_{\perp}(d)+\alpha'_{\parallel}(d)]=0.5$ found for hydrocarbons.[22,23]

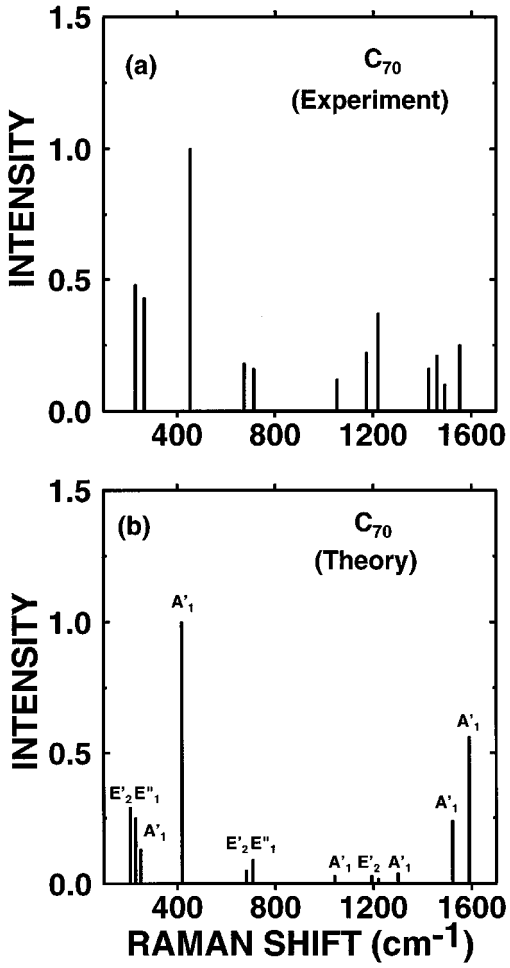

FIG. 5. (a) Experimental Raman intensities of C_{70} obtained by Chase, Herron, and Holler (Ref. 24). (b) Calculated intensities of Raman active modes in C_{70}, using first-principles eigenvectors and eigenfrequencies of Adams, Page, and Sankey (Ref. 39). The bond polarizability parameters used are the same as for C_{60}, with a cutoff between ''single'' and ''double'' bonds at 1.425 Å. In both (a) and (b), the Raman intensities have been normalized to the A_1' peak in the 400-cm^{-1} region.

Figure 4(b) shows the Raman intensity from just the second term in Eq. (4). As anticipated, the high-energy H_g modes contribute preferentially to this term. The contributions of $H_g(1)$, $H_g(2)$, and $H_g(3)$ are seen to be very small, with the latter two being vanishingly weak in the scale of the figure. The relative intensities within this panel can be changed somewhat by allowing for different parameters for single and double bonds, but the effect is much less dramatic in comparison with the A_g case in Fig. 4(a).

Figure 4(c) represents the Raman intensity from just the bond rotation contribution (third term) in Eq. (4). The low-energy $H_g(1)$ mode is seen to give the strongest peak. Interestingly, we again find that $H_g(2)$ and $H_g(3)$ are predicted to be very weak. These modes acquire an intensity comparable to the experimental values only when the anisotropy parameter $\alpha_\parallel - \alpha_\perp$ is allowed to take different values for single and double bonds.

It appears from Figs. 4(b) and 4(c) that $H_g(8)$ should be one of the strongest Raman modes. This is not the case, as shown in Fig. 3. The reason is that the contributions of this mode to the second and third terms of Eq. (4) have opposite signs. Since these terms must be added before the entire expression is squared, we obtain a partial cancellation. This destructive interference is most dramatic for $H_g(8)$, but also occurs for the other H_g modes, with the exception of $H_g(1)$ and $H_g(5)$. In view of the strong cancellation for $H_g(8)$, the discrepancy between experiment and *ab initio* predictions[15] for the intensity of this mode is not surprising.

We now return to the observed discrepancies between Raman polarizability parameters for C_{60} and the hydrocarbons ethane and ethylene. As explained above, the average value of the bond anisotropy becomes smaller in our fit relative to the average value of the trace derivatives. This has the effect of reducing the intensity of $H_g(1)$ relative to $A_g(1)$, as needed from a comparison of the predicted and observed Raman spectra in Fig. 1. On the other hand, the fit ratio $[\alpha_\parallel(s)-\alpha_\perp(s)]/[\alpha_\parallel(d)-\alpha_\perp(d)]$, which is four times larger than for hydrocarbons, is determined by the intensities of the $H_g(2)$ and $H_g(3)$ modes relative to $H_g(1)$. It is interesting to note that the contributions of $H_g(2)$ and $H_g(3)$ to the second term of Eq. (4) are found to remain very small in Fig. 4. Hence the relative intensity of these two peaks is approximately fixed, once we fit the relative intensity between either of these modes and $H_g(1)$ by adjusting the ratio $[\alpha_\parallel(s)-\alpha_\perp(s)]/[\alpha_\parallel(d)-\alpha_\perp(d)]$. We predict a relative intensity of unity between $H_g(2)$ and $H_g(3)$, whereas experiment indicates that $H_g(2)$ is roughly four times stronger than $H_g(3)$. These results clearly indicate a limitation of the simple bond polarizability model that we have used. It is possible that our assumption of cylindrical symmetry for the bond polarizabilities and the use of the ''zero-order'' approximation are not justified for the prediction of the weak Raman peaks in C_{60}. Thus, the difference between our fit ratio $[\alpha_\parallel(s)-\alpha_\perp(s)]/[\alpha_\parallel(d)-\alpha_\perp(d)]$ for C_{60} and that for hydrocarbons may not have any profound physical significance, but may simply reflect our attempt to account for the measured intensities of $H_g(2)$ and $H_g(3)$ relative to $H_g(1)$ within these approximations.

The second significant discrepancy between our result for C_{60} and hydrocarbons concerns the trace derivative ratio $[2\alpha'_\perp(s)+\alpha'_\parallel(s)]/[2\alpha'_\perp(d)+\alpha'_\parallel(d)]$, which determines the relative intensity between $A_g(1)$ and $A_g(2)$. Since these are the strongest peaks observed in the Raman spectrum, we expect to account for their intensities in terms of our simple bond polarizability model. It is therefore quite surprising that the trace derivative ratio is found to be smaller in C_{60} than in hydrocarbons. The measured single- and double-bond lengths in C_{60} differ by only 0.05 Å, whereas the carbon-carbon bond-length difference between ethane and ethylene is 0.14 Å. Thus one might expect for C_{60} a trace derivative ratio closer to 1. On the other hand, the screening corrections[35] referred to in Sec. I depend on the average molecular radius, which changes for the $A_g(1)$ breathing mode but remains constant, to first order, for the pentagonal pinch $A_g(2)$ mode. Thus the dynamical screening effects may be different for the two totally symmetric Raman modes in C_{60}. In a bond polarizability fit such as carried out here, these differences would be included in an effective manner by adjusting the trace derivative ratio. Hence our small fit value for this ratio may not represent a physical difference at the individual bond level. It is clear that more studies are needed to clarify this issue; in particular, absolute Raman intensities from C_{60} in the gas phase would be very useful for a final assessment of the bond polarizability model.

C. Transferability of the C_{60} fit Raman parameters to C_{70}

The Raman spectrum of C_{70} has been recalculated using the C_{60} fit parameters from Table I. For this calculation, we used the approach discussed earlier to partition the C_{70} bonds into a ''single-bond'' group and a ''double-bond'' group. As in the earlier calculations, we again find that the best bond-length cutoff is 1.425 Å. The resulting spectrum is compared with experimental data in Fig. 5. We note that the effect of the C_{60} fit parameters on the predicted C_{70} Raman spectrum is qualitatively similar to the changes observed between the C_{60} Raman spectrum calculated with hydrocarbon parameters and the fit C_{60} Raman spectrum. The intensity of the three low-energy peaks is reduced relative to the A'_1 mode near 400 cm^{-1}. However, this relative intensity is overcorrected, resulting in a larger discrepancy with experiment than in the calculation with hydrocarbon parameters (Fig. 2). The high-energy peaks gain in intensity relative to the peaks below 500 cm^{-1}, as in the C_{60} case. Some of the peaks in the 1000–1200-cm^{-1} region are now predicted to have observable intensities, in analogy with C_{60} H_g peaks in the same range. However, these intensities are still too weak compared with experiment. Also, while the predicted strong peaks at high energies belong to the A'_1 representation, there is no convincing experimental evidence[24] that any of the peaks observed beyond 1400 cm^{-1} belong to this representation.

Owing to the lower symmetry of C_{70}, the three terms of Eq. (4) do not lead to a natural separation between the contributions from totally symmetric modes and those from the other Raman-active modes. In particular, since the total static polarizability of C_{70} is anisotropic, the contributions from the A'_1 modes are not limited to the first term, as was the case with the totally symmetric modes in C_{60}. This makes it difficult to analyze the relative contributions of different parameters to the Raman spectrum of C_{70}. We have noticed, however, that significant improvements of the theoretical prediction in Fig. 5(a) can be obtained by further adjusting the value of $2\alpha'_\perp+\alpha'_\parallel$ for the shortest pentagonal bond and for the longest hexagonal bond. In this manner, we obtain reasonable intensities for the modes above 1000 cm^{-1}. However, the theoretical spectrum in this region is dominated by totally symmetric modes, for which there is scarce experimental evidence, as noted above.

It is apparent from the above discussion that the use of the C_{60} fit parameters does not lead to a dramatic improvement of the predicted C_{70} Raman spectrum, compared to the pre-

diction using C_{60} hydrocarbon parameters. This is perhaps to be expected in view of the cancellations discussed earlier for H_g modes in C_{60} and the crude partitioning of bonds in C_{70} into ''single'' and ''double'' groups. In particular, the observation that the Raman spectra depend strongly on the derivatives of the trace polarizability for each bond clearly highlights the limitations of this approach. On the other hand, the fact that the effect of the Raman polarizability parameters is similar for C_{60} and C_{70} suggests that the transferability scheme for fullerenes may be improved if the bond polarizability parameters are obtained by fitting to the Raman spectra of a wider class of fullerenes than just C_{60}. Unfortunately, as mentioned above, only the Raman spectrum of C_{60} can be fit at this point, due to the uncertainties in the mode assignments for all other fullerenes.

IV. CONCLUSIONS

We have shown that the static polarizabilities of C_{60} and C_{70} are in good agreement with the predictions of a bond polarizability model, using hydrocarbon bond polarizability parameters. When the model is extended to the calculation of the C_{60} and C_{70} Raman spectra, we find good agreement with the experimental intensities for low-energy modes, but significant discrepancies for high-energy modes. We then fit the bond polarizability model to the Raman spectrum of C_{60} and obtain very good agreement with experiment. The resulting fit parameters are used to predict the Raman spectrum of C_{70} and the results are compared with the C_{70} predictions based on hydrocarbon parameters. The hydrocarbon parameters are somewhat better than the C_{60} fit parameters for the description of C_{70} peak intensities below 1000 cm^{-1}, whereas the C_{60} fit parameters give better agreement with experiment for the C_{70} high-energy Raman peaks. Our results suggest that calculations of the Raman spectra of other fullerenes, using either hydrocarbon polarizability parameters or parameters fit to C_{60} should lead to good agreement with peaks below 1000 cm^{-1}. Higher-energy modes are expected to be better reproduced by the C_{60} fit parameters, but the uncertainties may be larger in this range. An application of this method—using the bond partitioning approach described here for C_{70}—has been presented by Adams and Page for the case of photopolymerized C_{60} and for C_{119} (Ref. 45).

ACKNOWLEDGMENTS

We would like to thank B. Chase for the experimental Raman data and S. Montero for extensive correspondence on the polarizability parameters for hydrocarbons. Useful discussions with M. Cardona are also acknowledged. This work was supported by the National Science Foundation under Grant Nos. DMR-9058343, DMR-9521507, and DMR-9510182.

[1] W. Krätschmer, L. D. Lamb, K. Fostiropoulos, and D. R. Huffman, Nature **347**, 354 (1990).
[2] D. S. Bethune, G. Meijer, W. C. Tang, and H. J. Rosen, Chem. Phys. Lett. **174**, 219 (1990).
[3] G. Dresselhaus, M. S. Dresselhaus, and P. C. Eklund, Phys. Rev. B **45**, 6923 (1992).
[4] Z. Hricha, J. L. Sauvajol, J. M. Lambert, and A. Zahab, Solid State Commun. **90**, 723 (1994).
[5] S. P. Love, D. McBranch, M. I. Salkola, N. V. Coppa, J. M. Robinson, B. I. Swanson, and A. R. Bishop, Chem. Phys. Lett. **225**, 170 (1994).
[6] P. J. Horoyski, M. L. W. Thewalt, and T. R. Anthony, Phys. Rev. Lett. **74**, 194 (1995).
[7] P. H. M. van Loosdrecht, P. J. M. van Bentum, and G. Meijer, Phys. Rev. Lett. **68**, 1176 (1992).
[8] M. Matus, H. Kuzmany, and W. Krätschmer, Solid State Commun. **80**, 839 (1991).
[9] V. N. Denisov, B. N. Marvin, G. Ruani, R. Zamboni, and C. Taliani, Zh. Eksp. Teor. Fiz. **102**, 300 (1992) [Sov. Phys. JETP **75**, 156 (1992)].
[10] K. Sinha, J. Menéndez, R. C. Hanson, G. B. Adams, J. B. Page, O. F. Sankey, L. D. Lamb, and D. R. Huffman, Chem Phys. Lett. **186**, 287 (1991).
[11] A. M. Rao, P. Zhou, K.-A. Wang, G. T. Hager, J. M. Holden, Y. Wang, W.-T. Lee, X.-X. Bi, P. C. Eklund, D. S. Cornett, M. A. Duncan, and I. J. Amster, Science **259**, 955 (1993).
[12] R. C. Haddon, A. F. Hebbard, M. J. Rosseinsky, D. W. Murphy, S. J. Duclos, K. B. Lyons, B. Miller, J. M. Rosamilia, R. M. Fleming, A. R. Kortan, S. H. Glarum, A. V. Makhija, A. J. Muller, R. H. Eick, S. M. Zahurak, R. Tycko, G. Dabbagh, and F. A. Thiel, Nature **350**, 320 (1991).
[13] P. Zhou, K.-A. Wang, P. C. Eklund, G. Dresselhaus, and M. S. Dresselhaus, Phys. Rev. B **48**, 8412 (1993).
[14] P. C. Eklund, P. Zhou, K.-A. Wang, G. Dresselhaus, and M. S. Dresselhaus, Phys. Rev. B **45**, 6234 (1992).
[15] P. Giannozzi and S. Baroni, J. Chem. Phys. **100**, 8537 (1994).
[16] G. B. Adams, J. B. Page, O. F. Sankey, and M. O'Keeffe, Phys. Rev. B **50**, 17 471 (1994); G. B. Adams, J. B. Page, O. F. Sankey, K. Sinha, J. Menéndez, and D. R. Huffman, *ibid.* **44**, 4052 (1991).
[17] A. A. Quong, M. R. Pederson, and J. L. Feldman, Solid State Commun. **87**, 535 (1993).
[18] V. P. Antropov, O. Gunnarsson, and A. I. Liechtenstein, Phys. Rev. B **48**, 7651 (1993).
[19] D. W. Snoke and M. Cardona, Solid State Commun. **87**, 121 (1993).
[20] D. Bermejo, S. Montero, M. Cardona, and A. Muramatsu, Solid State Commun. **42**, 153 (1982).
[21] F. Orduna, C. Domingo, S. Montero, and W. F. Murphy, Mol. Phys. **45**, 65 (1982).
[22] J. Martín and S. Montero, J. Chem. Phys. **80**, 4610 (1984).
[23] M. F. Orduna, A. del Olmo, C. Domingo, and S. Montero, J. Mol. Struc. **142**, 201 (1986).
[24] B. Chase, N. Herron, and E. Holler, J. Phys. Chem. **96**, 4262 (1992).
[25] M. Volkenstein, Dokl. Akad. Nauk. SSSR **32**, 185 (1941).
[26] For discussions see, for example, J. J. C. Teixeira-Dias and J. N. Murrel, Mol. Phys. **19**, 329 (1970), and K. M. Gough, J. Chem. Phys. **91**, 2424 (1989).
[27] S. L. Ren, Y. Wang, A. M. Rao, E. McRae, J. M. Holden, T. Hager, K.-A. Wang, W.-T. Lee, H. F. Ni, J. Selegue, and P. C.

Eklund, Appl. Phys. Lett. **59**, 2678 (1991).
[28] P. Eklund, Bull. Am. Phys. Soc. **37**, 191 (1992).
[29] T. K. Bose, J. S. Sochanski, and R. H. Cole, J. Chem. Phys. **57**, 3592 (1972).
[30] M. P. Bogaard, A. D. Buckingham, R. K. Pierens, and A. H. White, J. Chem. Soc. Faraday Trans. 1 **74**, 3008 (1978).
[31] G. W. Hills and W. Jeremy Jones, J. Chem Soc. Faraday Trans. 2 **71**, 812 (1975).
[32] A. A. Quong and M. R. Pederson, Phys. Rev. B **46**, 12 906 (1992).
[33] B. Shanker and J. Applequist, J. Phys. Chem. **98**, 6846 (1994).
[34] S.-L. Ren, K.-A. Wang, P. Zhou, Y. Wang, A. M. Rao, M. S. Meier, J. P. Selegue, and P. C. Eklund, Appl. Phys. Lett. **61**, 124 (1992).
[35] Y. Wang, G. F. Bertsch, and D. Tománek, Z. Phys. D **25**, 181 (1993).
[36] G. W. Chantry, in *The Raman Effect*, edited by A. Anderson (Dekker, New York, 1971), Vol. 1, p. 49.
[37] See, for example, L. M. Sverdlov, M. A. Kovner, and E. P. Krainov, *Vibrational Spectra of Polyatomic Molecules* (Wiley, Jerusalem, 1974), and references therein.
[38] J. Kulda, D. Strauch, P. Pavone, and Y. Ishii, Phys. Rev. B **50**, 13 347 (1994).
[39] G. B. Adams, J. B. Page, and O. F. Sankey (unpublished).
[40] J. A. Salthouse and M. J. Ware, *Point Group Character Tables and Related Data* (Cambridge University Press, Cambridge, 1972).
[41] R. A. Jishi, M. S. Dresselhaus, G. Dresselhaus, K.-A. Wang, P. Zhou, A. M. Rao, and P. C. Eklund, Chem. Phys. Lett. **206**, 187 (1993).
[42] S. Guha, J. Menéndez, J. B. Page, G. B. Adams, G. S. Spencer, J. P. Lehman, P. Giannozzi, and S. Baroni, Phys. Rev. Lett. **72**, 3359 (1994).
[43] Eigenvectors and eigenfrequencies are used to compute Raman spectra, using Eq. (4). Each peak is assigned the experimental linewidth of ~ 5 cm^{-1} quoted in Ref. (24). (This is much larger than the natural linewidth of the peaks at low temperatures, as reported in Ref. 42.) The spectra are then averaged according to the natural abundance of ^{13}C. We find that the resulting spectra differ negligibly from the corresponding spectra predicted for isotopically pure molecules. Thus, the isotope effect does not affect the comparison between predictions and experiment in Figs. 1 and 2.
[44] S. Sanguinetti, G. Benedek, M. Righetti, and G. Onida, Phys. Rev. B **50**, 6743 (1994).
[45] G. B. Adams and J. B. Page, in Fullerene Polymers and Polymer Composites, edited by P. C. Eklund and A. M. Rao (Springer-Verlag, Berlin, in press).